⌘ *Author's Choice*

THE JOURNAL OF BIOLOGICAL CHEMISTRY VOL. 284, NO. 13, pp. 8855–8865, March 27, 2009

β-Arrestin-2 Mediates Anti-apoptotic Signaling through Regulation of BAD Phosphorylation*[S]

Received for publication, November 6, 2008, and in revised form, January 12, 2009 Published, JBC Papers in Press, January 26, 2009, DOI 10.1074/jbc.M808463200

Seungkirl Ahn[‡], Jihee Kim[‡], Makoto R. Hara[‡], Xiu-Rong Ren[‡], and Robert J. Lefkowitz[‡§¶1]

From the Departments of [‡]Medicine and [§]Biochemistry and [¶]Howard Hughes Medical Institute, Duke University Medical Center, Durham, North Carolina 27710

β-Arrestins, originally discovered as terminators of G protein-coupled receptor signaling, have more recently been appreciated to also function as signal transducers in their own right, although the consequences for cellular physiology have not been well understood. Here we demonstrate that β-arrestin-2 mediates anti-apoptotic cytoprotective signaling stimulated by a typical 7-transmembrane receptor the angiotensin ATII 1A receptor, expressed endogenously in rat vascular smooth muscle cells or by transfection in HEK-293 cells. Receptor stimulation leads to concerted activation of two pathways, ERK/p90RSK and PI3K/AKT, which converge to phosphorylate and inactivate the pro-apoptotic protein BAD. Anti-apoptotic effects as well as pathway activities can be stimulated by an angiotensin analog (SII), which has been previously shown to activate β-arrestin but not G protein-dependent signaling, and are abrogated by β-arrestin-2 small interfering RNA. These findings establish a key role for β-arrestin-2 in mediating cellular cytoprotective functions by a 7-transmembrane receptor and define the biochemical pathways involved.

β-Arrestins 1 and 2 were originally identified as signal terminators for G protein-dependent 7-transmembrane receptor (7TMR)[2] signaling. Their binding to the receptor sterically inhibits receptor coupling to G protein leading to inactivation of effectors such as second messenger generating enzymes (1). Besides this classical function, recently accumulating evidence has revealed novel functions of β-arrestins as signal transducers in various signaling pathways (2). Among other processes, β-arrestins have been suggested to play a role in regulation of cell death, but this area has been controversial and largely devoid of mechanistic insight. There have been reports implicating β-arrestins in both pro- and anti-apoptotic responses as well as in non-apoptotic cell death (3–10). For example, it has been shown that stimulation of a number of 7TMRs including the *N*-formyl peptide receptor induces apoptosis in β-arrestin 1/2 double knock-out mouse embryonic fibroblasts, and that reintroduction of either β-arrestin-1 or -2 completely prevents this apoptosis (5). Conversely, β-arrestins also have been reported to mediate cell death. β-Arrestin-2, particularly a dephosphorylated form, has been shown to facilitate inhibition of NF-κB activation in response to UV, leading to promotion of UV-induced cell death (8).

Bcl-2 family proteins are known to determine the outcome of an intrinsic apoptotic process initiated by release of cytochrome *c* and apoptotic factors from the mitochondria (11). BAD, a BH3-only protein is one of the "death-promoting" members of the Bcl-2 family and its pro-apoptotic activity is regulated primarily by phosphorylation at several sites (12, 13). Survival factors induce BAD phosphorylation via several protein kinase signaling pathways (13) including activation of mitogen-activated protein kinase (MAPK)-ribosomal S6 kinase (RSK) (14–16) and phosphatidylinositol 3-kinase (PI3K)-AKT (17, 18). Phosphorylated BAD associates with 14-3-3 proteins in the cytoplasm, preventing translocation of BAD to the mitochondria (19) and its interaction with the anti-apoptotic proteins Bcl-xL and Bcl-2 (13, 20). These proteins, freed from BAD, in turn associate with two other pro-apoptotic proteins, BAX and BAK. Such association prevents aggregation of these pro-apoptotic proteins on the mitochondrial membrane, stopping cytochrome *c* release and consequently inhibiting apoptosis (11, 20).

Recently several 7TMRs have been shown to activate the extracellular signal-regulated kinase (ERK) MAPK cascade and PI3K-AKT pathways in a β-arrestin-dependent manner (2). In particular, it has been demonstrated that β-arrestin-mediated ERK activation by angiotensin II type 1A (AT_{1A}) (21, 22), vasopressin V_2 (23), parathyroid hormone (24), and β_2-adrenergic receptors (25) is G protein-independent. Furthermore, we have previously found that β-arrestin-mediated ERK activation is quite distinct in its temporal (22–25) and spatial (22, 26) patterns from ERK-activated via G protein-dependent stimulation. In the case of AT_{1A}R-mediated ERK activation in receptor-transfected human embryonic kidney (HEK)-293 cells, for example, the G protein-dependent activation is rapid, quite transient (peak at 2–5 min), and leads to nuclear translocation of the activated ERK. In contrast, β-arrestin-2-dependent ERK activation is slower, quite persistent, and entirely confined to the cytoplasm, particularly to endosomal vesicles (22). Such

* This work was supported, in whole or in part, by National Institutes of Health Grants HL16037 and HL70631. The costs of publication of this article were defrayed in part by the payment of page charges. This article must therefore be hereby marked "*advertisement*" in accordance with 18 U.S.C. Section 1734 solely to indicate this fact.

⌘ *Author's Choice*—Final version full access.

[S] The on-line version of this article (available at http://www.jbc.org) contains supplemental Figs. S1 and S2.

[1] Investigator with the Howard Hughes Medical Institute. Founder of Trevena Inc., all other authors declare no competing financial interest. To whom correspondence should be addressed. Tel.: 919-684-2974; Fax: 919-684-8875; E-mail: lefko001@receptor-biol.duke.edu.

[2] The abbreviations used are: 7TMR, 7-transmembrane receptor; AngII, angiotensin II; AT_1R, angiotensin II type 1 receptor; ERK, extracellular signal-regulated kinase; HEK, human embryonic kidney; MAPK, mitogen-activated protein kinase; PI3K, phosphatidylinositol 3-kinase; PKC, protein kinase C; RSK, ribosomal S6 kinase; SII, [Sar^1,Ile^4,Ile^8]angiotensin II; siRNA, small interfering RNA; VSMC, vascular smooth muscle cell; Z, benzyloxycarbonyl; fmk, fluoromethyl ketone; PBS, phosphate-buffered saline.

differences in ERK activation strongly imply that there must be subsets of ERK targets and physiological outcomes differentially regulated through β-arrestin *versus* G protein-dependent mechanisms. In the case of AKT activation, stimulation of 7TM protease-activated receptors with thrombin has been shown to activate AKT in a β-arrestin-1-dependent manner (27). Stimulation of the AT_1 receptor also has been shown to activate AKT in several cell types including vascular smooth muscle cells (VSMCs) (28, 29) although it has not been determined whether β-arrestins are involved in this signaling.

Accordingly, the studies reported here were undertaken to examine the role of β-arrestin in 7TMR-regulated apoptosis and to determine the downstream pathways mediating this regulation in a physiologically relevant non-transfected cellular receptor system. For this purpose, we chose the AT_1 receptor in rat VSMCs.

EXPERIMENTAL PROCEDURES

Materials—[Sar^1,Ile^4,Ile^8]AngII (Sar-Arg-Val-Ile-Ile-His-Pro-Ile) (SII) was synthesized as described (21, 30). GF109203X (GFX), Ro-31-8425, U0126, and Z-VAD-fmk were purchased from Calbiochem. SL0101 was from Toronto Research Chemicals (North York, Ontario, Canada). All other reagents were purchased from Sigma, unless otherwise described. Plasmids expressing hemagglutinin-tagged wild-type, S112A and S136A mutant BAD were a generous gift from Dr. Michael E. Greenberg (Harvard Medical School).

Antibodies—Rabbit polyclonal phospho-AKT (Ser^{473}) (used in an 1:1,000 dilution for immunoblotting), AKT (1:2,000), phospho-BAD (Ser^{112}) (1:500–1,000), BAD (1:1,000 for human BAD), Bcl-xL (1:1,000), caspase-3 (1:1,000), cleaved caspase-3 (Asp^{175}) (1:1,000), phospho-ERK1/2 (Thr^{202}/Tyr^{204}) (1:2,000), and phospho-p90RSK (Thr^{359}/Ser^{363}) (1:500–1,000) antibodies were purchased from Cell Signaling (Danvers, MA). Polyclonal 14-3-3β (C-20) (1:1,000), RSK-1 (C-21) (1:1,000), and mouse monoclonal BAD (C-7) (1:1,000 for human BAD) antibodies were from Santa Cruz (Santa Cruz, CA). Monoclonal BAD (1:2,000 for rat BAD) and polyclonal ERK1/2 (1:10,000) antibodies were from BD Transduction Laboratories (Franklin Lakes, NJ) and Millipore (Billerica, MA), respectively. Human and rat β-arrestins were detected by A1CT and A2CT antibodies, respectively (31).

Synthesis of Small Interfering RNAs (siRNAs)—Chemically synthesized, double-stranded siRNAs, with 19-nucleotide duplex RNA and 2-nucleotide 3′-dTdT overhangs were purchased from Dharmacon (Lafayette, CO) in deprotected and desalted forms. The two different siRNA sequences targeting human (rat) β-arrestin-2 were 5′-GGACCGC(G)AAAGUGUUUGUG-3′ and 5′-CCAACCUCAUUGAAUUU(C)GA-3′, corresponding to positions 150–168 and 1112(1115)-1131(1133), relative to the start codon, respectively (32). A non-silencing RNA duplex (5′-UUCUCCGAACGUGUCACGU-3′), as the manufacturer (Xeragon, Germantown, MD) indicated, was used as a control.

Cell Culture and Transfection—VSMCs were isolated from aorta of male Sprague-Dawley rats and maintained as described (32). Eight to 90% confluent early passage (<5) VSMCs were transfected with siRNA using the Lipofectamine 2000 transfection reagent (Invitrogen) according to the modified manufacturer's instructions. Briefly, 60 μl of the Lipofectamine 2000 transfection reagent was added to 300 μl of the medium-199 and 20 μg of siRNA was added to 400 μl of the medium. Both solutions were allowed to stand 5–10 min at room temperature and mixed by inversion. Following a 15–20-min incubation at room temperature, the entire transfection mixture was added to VSMCs in a 100-mm dish containing 5 ml of the fresh, serum-free medium. After cells were incubated for overnight at 37 °C, an additional 5 ml of the medium with 20% fetal bovine serum and 2% penicillin/streptomycin were added to the dish. Following an additional incubation for 24 h, cells were divided into 6-well plates or 35-mm glass bottom dishes (MatTek, Ashland, MA) for further procedures. For DNA transfection into VSMCs in either 35-mm glass bottom dishes or 6-well plates, the Lipofectamine LTX transfection reagent (Invitrogen) was used with the PLUS reagent (Invitrogen) according to the manufacturer's instructions. HEK-293 cells, stably expressing AT_{1A} receptors (~600 fmol/mg of proteins), were established after transfection with a zeocin-resistant AT_{1A} receptor expression plasmid using FuGENE 6 (Roche) according to the manufacturer's instructions. Stable clones were selected in the presence of zeocin (300 μg/ml) (Invitrogen). Cells were maintained and transfected with siRNAs using GeneSilencer (Genlantis, San Diego, CA) as described (22).

Cleaved Caspase-3 and DNA Fragmentation Assays—VSMCs were serum-starved for ~24 h and then stimulated with 100 nM AngII or 10 μM SII at 37 °C for 5 min prior to treatment with either 80 μM H_2O_2 or 50 μM etoposide. After a further incubation overnight, cell lysates were prepared. Pro- and cleaved caspase-3 were visualized, and the amounts of cleaved caspase-3 were quantified as described for immunoblotting in this section. The amounts of fragmented DNA were measured by the enzyme-linked immunosorbent assay using the Cell Death Detection ELISA^{PLUS} kit (Roche) according to the manufacturer's instructions.

Immunostaining—VSMCs on 35-mm glass bottom dishes were fixed with 5% formaldehyde diluted in phosphate-buffered saline (PBS). Fixed cells were permeabilized by incubation with 0.2% Triton X-100 in PBS for 20 min. After blocking with 2% bovine serum albumin in PBS for 1 h, cells were incubated with the mouse monoclonal anti-cytochrome *c* (BD Pharmingen, 1:100) antibody at room temperature for 2 h, and repeatedly washed with PBS. Next, incubation of the Bodipy fluorescein-conjugated secondary antibody (Molecular Probes, 1:100) was done for 1 h at room temperature followed by repeated washes with PBS. For subsequent staining of the hemaglutinin epitope-tagged BAD, cells were incubated with a polyclonal hemaglutinin probe (Y11) antibody (Santa Cruz, 1:200) at room temperature overnight. The Texas Red-conjugated secondary antibody (Molecular Probes, 1:250) was then added for 1 h. Confocal images were obtained on a Zeiss LSM510 laser scanning microscope using single line (488 nm) or multitrack sequential excitation (488 and 568 nm) and emission (515–540 nm, Bodipy fluorescein; 585–615 nm, Texas Red) filter sets.

Immunoblotting and Immunoprecipitation—In most cases, cellular extracts from VSMCs or HEK-293 cells on 6-well plates were prepared as described previously (22). For caspase-3 immunoblotting, VSMC lysates were prepared using the RIPA

lysis buffer. Equal amounts (~10 μg) of cellular extracts/lysates were used for immunoblotting performed as described previously (22). For immunoprecipitation, lysates form HEK-293 cells in 100-mm dishes were prepared using the glycerol/Nonidet P-40 lysis buffer (33). Equal amounts of cell lysates (300–500 μg of total protein in 1 ml of the buffer) were incubated with 1–2 μg of either rabbit polyclonal 14-3-3 β (C-20) or mouse monoclonal BAD (C-7) antibody and protein A- or G-agarose beads, respectively, overnight at 4 °C. Co-immunoprecipitated proteins were detected by immunoblotting. Each band in immunoblots was quantified by densitometry using the GeneTools program (SynGene).

Statistical Analysis—Statistical significance in bar graphs was determined by using a one-way analysis of variance (PRISM software) to correct for multiple comparisons (Bonferroni's multiple comparison test) or *t* test for single comparisons between AngII or SII-stimulated *versus* non-stimulated in a certain condition, unless otherwise indicated in each figure. Statistical significance in each time point of kinetic graphs was determined by using a two-way analysis of variance (Bonferroni's post-test) between β-arrestin-2 siRNA-transfected and control cells. *p* value (*, $p < 0.05$; **, $p < 0.01$; ***, $p < 0.001$) of <0.05 was considered statistically significant.

RESULTS

β-Arrestin-2 Is Essential for the Anti-apoptotic Effects of AngII on Primary Cultured Vascular Smooth Muscle Cells—It has been previously reported that the octapeptide hormone angiotensin II (AngII) promotes anti-apoptotic effects in VSMCs through AngII type 1 receptors (AT_1Rs) (34, 35). We and others have previously found that β-arrestin-2 is the isoform that mediates $AT_{1A}R$-activated ERK signaling (33, 36), which is potentially an anti-apoptotic pathway. We have also found that β-arrestin-1 functionally opposes this signaling (33). Consequently, we used VSMCs to explore the role of β-arrestin-2 in regulating apoptosis. We first monitored the effects of AngII stimulation on the activation of caspase-3 (cleavage of procaspase-3) induced by apoptotic challenges in VSMCs transfected with either control or β-arrestin-2 siRNAs. We used 100 nM AngII to obtain maximal responses in this assay. It has been previously reported that AngII-stimulated ERK activation reaches maximal levels with this concentration in HEK-293 cells transiently expressing $AT_{1A}R$ (33). Apoptotic stimulation by either hydrogen peroxide (H_2O_2) (Fig. 1*A*) or etoposide (Fig. 1*B*) dramatically increases the level of cleaved caspase-3 in control VSMCs. The levels of cleaved caspase-3 induced by such apoptotic stimuli were reduced to ~50% by AngII pretreatment (Fig. 1, *C* and *D*). Next, we examined the effects of siRNA-mediated β-arrestin-2 knock-down on AngII-promoted protection from caspase-3 cleavage. Depletion of β-arrestin-2 not only leads to increases (up to ~150%) in the induction of cleaved caspase-3 levels by treatment with hydrogen peroxide or etoposide, but also eliminates AngII-mediated decreases in these levels (Fig. 1, *C* and *D*). On the other hand, knocking-down β-arrestin-1 leads to decreases in apoptotic reagent-induced caspase-3 cleavage even in the absence of stimulation with AngII, which is similar in extent to the protection observed in AngII-treated control cells. Stimulation with AngII results in no significant further protection in cells knocked down for β-arrestin-1 (data not shown). These results suggest an essential role of β-arrestin-2 in AngII-stimulated protection from caspase-dependent apoptotic processes.

Because the release of cytochrome *c* from mitochondria is one of the key upstream events for the coordinated activation of caspases (34, 37), we next examined effects of AngII stimulation on the hydrogen peroxide-induced redistribution of cytochrome *c* in control or β-arrestin-2 siRNA-transfected VSMCs. In the absence of an apoptotic challenge, cytochrome *c* is well distributed within cytoplasmic, mitochondrial networks in control cells (Fig. 1*E*, *upper left panel*). Treatment with hydrogen peroxide leads to the rearrangement of cytochrome *c* into a cytoplasmic dotted pattern in cells (Fig. 1*E*, *upper middle panel*). Hydrogen peroxide-induced redistribution of cytochrome *c* is largely reversed by prior stimulation with AngII (Fig. 1*E*, *upper right panel*). These staining patterns of cytochrome *c* are, in all cases, superimposed with that of the MitoTracker, a mitochondrial marker (supplemental Fig. S1), confirming that the changes in the staining patterns of cytochrome *c* shown in Fig. 1*E* indeed represent mitochondrial remodeling. Mitochondrial rearrangement and fragmentation have been observed in apoptotic cells, especially when apoptosis has been induced by pro-apoptotic members of the Bcl-2 family of proteins (38, 39). Depletion of β-arrestin-2 has no effect on mitochondrial network organization (Fig. 1*E*, *lower left panel*), and does not alter the pattern of fragmentation observed after hydrogen peroxide treatment (Fig. 1*E*, *lower middle panel*). However, unlike control siRNA-transfected cells, pre-stimulation with AngII fails to reverse the hydrogen peroxide-induced mitochondrial fragmentation in β-arrestin-2 siRNA-transfected cells (Fig. 1*E*, *lower right panel*). These results further support an important role for β-arrestin-2 in mediating AngII-stimulated anti-apoptotic activity.

To further validate these findings, we measured DNA fragmentation, a hallmark of cell death, in VSMCs transfected with either control or β-arrestin-2 siRNAs. Treatment with hydrogen peroxide (Fig. 1*F*) or etoposide (Fig. 1*G*) causes a 4–6-fold increase in DNA fragmentation. In control siRNA-transfected cells, pre-stimulation with AngII reduces (by ~40%) the extent of DNA fragmentation induced by both reagents (Fig. 1, *F* and *G*). On the contrary, we did not observe decreases in DNA fragmentation after pre-stimulation with AngII in β-arrestin-2 siRNA-transfected cells (Fig. 1, *F* and *G*), mirroring the situation observed with caspase-3 activation. In the case of β-arrestin-1 knock-down, effects on DNA fragmentation also mirror the effects observed with caspase-3 cleavage (data not shown). Taken together, these results demonstrate that β-arrestin-2 is crucial for AngII-stimulated protection of VSMCs from apoptotic cell death.

To establish whether the β-arrestin-2-dependent AT_1R-mediated inhibition of apoptotic processes can be accomplished in the absence of G protein activation, we stimulated VSMCs with an AngII analog, [Sar^1,Ile^4,Ile^8]AngII (SII). This mutant form of AngII was previously shown not to activate G proteins (21, 30). As shown in Fig. 1, *H* and *I*, stimulation of the cells with SII leads to significant decreases (35–45%) in the levels of cleaved caspase-3 upon hydrogen peroxide or etoposide treatment. The extent of DNA fragmentation induced by these reagents is also

reduced to a similar extent upon prestimulation with SII (Fig. 1*J*). The extent of SII-stimulated decreases (30–45%) in both assays is similar to those evoked by AngII stimulation (40–50%). This result demonstrates that activation of the AT_1 receptor elicits cytoprotective effects mainly through G protein-independent signaling.

β-Arrestin-2 Mediates Activation of ERK-RSK and AKT Signaling Pathways, Leading to Phosphorylation of BAD in AngII-stimulated VSMCs—Recently a growing list of biochemical pathways has been shown to be stimulated via 7TMRs through β-arrestin-dependent mechanisms (2). These include the ERK1/2 MAPKs (21–26) and AKT (27). Because both ERK and AKT signaling are reported to exert cytoprotective actions, we examined their possible involvement in the anti-apoptotic effects of AngII on VSMCs. Here we demonstrate that in VSMCs stimulated with AngII, ERK1/2 are activated, and this is significantly reduced by siRNA-mediated knock-down of β-arrestin-2 (Fig. 2, *A–C*). The reduction is observed only after a 2-min stimulation, suggesting that, as previously shown in HEK-293 cells (22), prior to that time activation proceeds exclusively through G protein-dependent mechanisms. Ribosomal S6 kinase (RSK) is a well known downstream kinase for ERK signaling and it mediates a variety of physiological responses including anti-apoptosis (40, 41). Furthermore, RSK is activated by phosphorylation in the cytoplasm (40, 41) where ERK activated by β-arrestin-dependent mechanisms is confined (22, 26). Moreover, our recent high throughput proteomics screening using the stable isotope labeling amino acid in cell culture method have revealed that the level of p90RSK phosphorylation is increased by SII stimulation in HEK-293 cells expressing the AT_{1A} receptor.[3] Accordingly, we next tested whether phosphorylation of p90RSK occurs upon stimu-

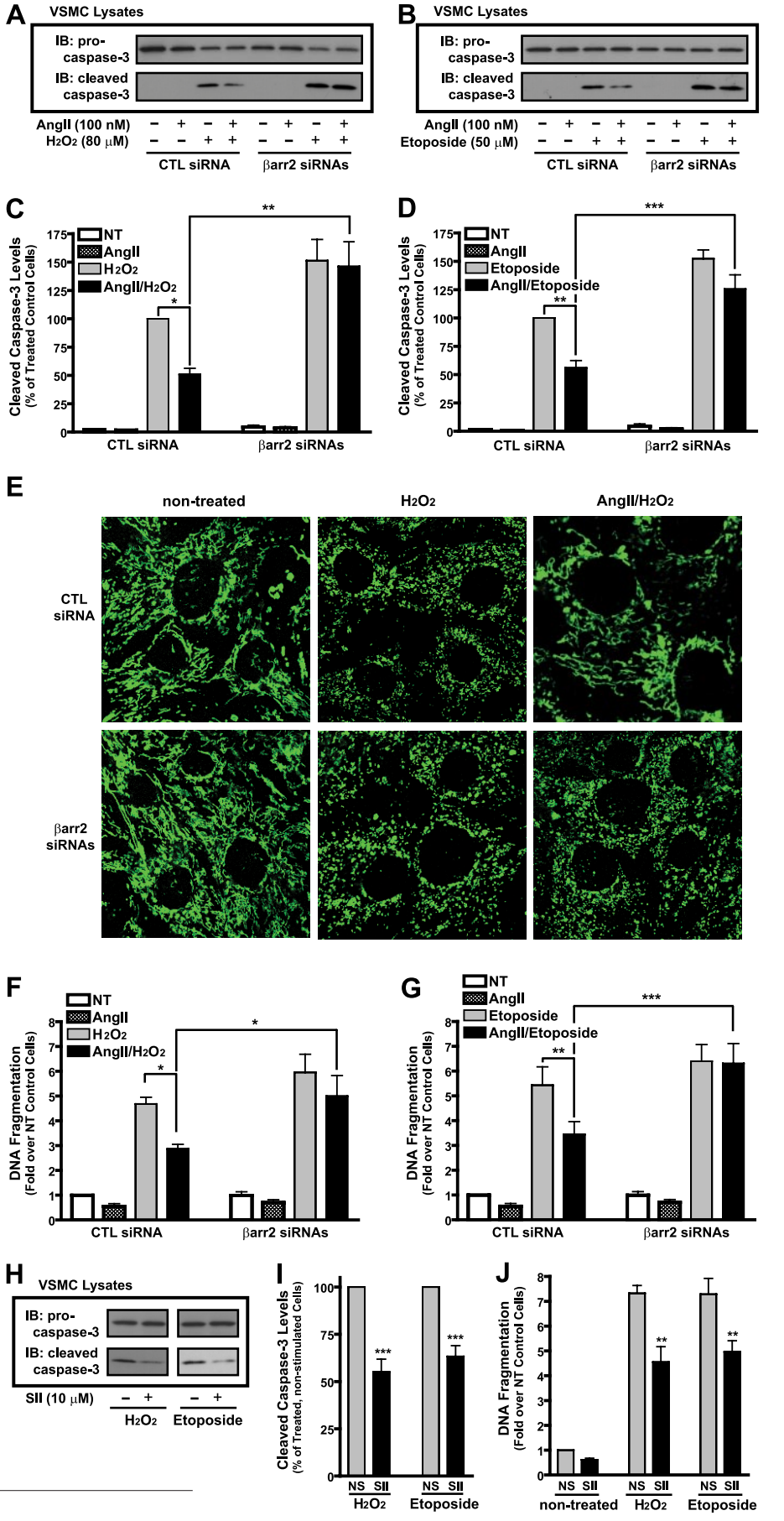

[3] S. Ahn and R. J. Lefkowitz, unpublished data.

lation with AngII and whether this is mediated by β-arrestin-2. As shown in Fig. 2, *D* and *E*, the kinetic pattern of AngII-stimulated p90RSK phosphorylation, particularly at ERK sites Thr^{359}/Ser^{363} (40, 41), is similar to that for ERK activation. In control siRNA-transfected cells, p90RSK phosphorylation also reaches a maximal level at 5 min after stimulation although it lags slightly behind ERK activation (compare 2-min points in Fig. 2, *C versus E*) and decreases gradually over 20 min. Silencing β-arrestin-2 expression leads to rapid and transient p90RSK phosphorylation, also similar to ERK activation. These results suggest that ERKs activated through both β-arrestin-2- and G protein-dependent pathways can phosphorylate RSK. However, β-arrestin-2-mediated phosphorylation of p90RSK is much slower and more prolonged than that due to activation of the β-arrestin-2-independent pathway, which is presumably G-protein-mediated.

RSK is also known to have many downstream targets mediating numerous physiological responses (40, 41). One such target is the pro-apoptotic protein BAD and its phosphorylation by RSK is known to inhibit its pro-apoptotic functions (14–16). Accordingly, we next examined phosphorylation of BAD at Ser^{113} (known to be a preferred RSK site) in VSMCs. In these cells, β-arrestin-2 RNA interference interestingly leads to almost complete attenuation in AT_1R-mediated BAD phosphorylation (Fig. 2, *F* and *G*). Taken together, our results suggest that AngII-induced RSK phosphorylation by ERK is partially mediated by β-arrestin-2- (especially >2 min) and G protein (<2 min)-dependent pathways. Nonetheless, it is predominantly RSK activated through the β-arrestin-2-mediated pathway that phosphorylates BAD upon activation of the AT_1 receptors in VSMCs.

To further validate the β-arrestin-2-dependent nature of the AT_1R-mediated activation of the ERK/p90RSK/BAD cascade, we stimulated the VSMCs with SII, which cannot activate G protein signaling. As shown in Fig. 2, *H* and *I*, SII stimulates both p90RSK and phosphorylation of BAD at the RSK site, thus confirming the G protein independence of these responses.

Another kinase that is known to phosphorylate and inactivate BAD leading to anti-apoptotic effects is AKT (17, 18). Moreover, β-arrestin-mediated activation of AKT has been demonstrated for 7TM protease-activated receptors (27) as well as for the receptor tyrosine kinase insulin-like growth factor 1 receptor (6). Accordingly, we tested the ability of AngII to promote phosphorylation of the stimulatory site, Ser^{473}, of AKT in the VSMCs. As shown in Fig. 2, *J* and *K*, time-dependent phosphorylation was observed, which was inhibited by β-arrestin-2 siRNAs at times later than 2 min of stimulation, indicating that this process is mediated in part by β-arrestin-2.

RSK- and AKT-mediated Phosphorylations of BAD Are Essential for AngII-stimulated Cell Protection—Our data suggest that RSK- and/or AKT-mediated phosphorylation of BAD might be a molecular mechanism that is responsible for the β-arrestin-2-mediated anti-apoptotic effects of AngII on VSMCs. To test this hypothesis, we first examined the effects of the RSK inhibitor SL0101 and the PI3K inhibitor LY294002, which is known to block AKT activation, on AngII-induced anti-apoptosis in VSMCs. Treatment with either SL0101 or LY294002 completely ablates the ability of AngII to protect against etoposide-induced apoptosis as assessed by either caspase-3 cleavage (Fig. 3, *A* and *C*) or DNA fragmentation (Fig. 3*D*). Fig. 3*B* shows that LY294002 blocks AngII-induced activation of AKT as assessed by phosphorylation of AKT Ser^{473}, and SL0101 blocks phosphorylation of BAD at the RSK site, BAD Ser^{113}. These results strongly support the thesis that β-arrestin-2 mediates AngII-stimulated cell protection by regulating RSK- and AKT-mediated phosphorylation of BAD. Moreover the concerted activation of both pathways appears to be necessary because blockade of either alone completely eliminates the anti-apoptotic effect.

To directly test whether RSK- and AKT-mediated phosphorylation of BAD are required for the anti-apoptotic actions of AngII, we studied the nature of overexpressed wild-type and phosphorylation-deficient mutants of BAD in VSMCs. We used the two mouse mutants BAD S112A and BAD S136A that are defective in RSK- and AKT-mediated phosphorylation, respectively (14, 18). Overexpression of wild-type BAD in the VSMCs leads to a typical apoptotic pattern of mitochondrial fragmentation as visualized by cytochrome *c* staining, whereas cells that do not express BAD show an intact mitochondrial architecture (Fig. 3*E*). Essentially identical images were obtained with the two mutant forms of BAD (supplemental Fig. S2), confirming the abilities of all these three forms of BAD to induce apoptosis upon overexpression.

Next we examined caspase-3 activation in cells expressing the three BAD constructs (Fig. 3, *F* and *G*). Despite relatively inefficient (<10%) transfection of the cells, robust increases in the levels of cleaved caspase-3 were observed in all cases (Fig. 3, *F* and *G*). In this system, AngII stimulation leads to partial but significant (~30%) decreases in these levels in cells overexpressing the wild-type BAD, whereas such reductions are not observed in cells expressing BAD S112A or BAD S136A (Fig. 3*G*). These results support the conclusion

FIGURE 1. **β-Arrestin-2, but not activation of G proteins, is essential for AngII-promoted cytoprotection against apoptotic challenges in rat VSMCs.** *A–G*, primary cultured VSMCs were transfected with either control (*CTL*) or simultaneously two different β-arrestin-2 (*βarr2*) siRNAs. *A* and *B*, cells were stimulated with AngII before either H_2O_2 (*A*) or etoposide (*B*) treatment as described under "Experimental Procedures." Pro- and cleaved caspase-3 were visualized by immunoblotting (*IB*). *C* and *D*, contents of cleaved caspase-3 in the immunoblots were quantified and expressed as percent of the level obtained in H_2O_2- (*C*) or etoposide- (*D*) treated cells in the absence of stimulation with AngII. Data represent the mean ± S.E. from at least five independent experiments. *E*, 50 μM Z-VAD-fmk was treated to block caspase-dependent cell death before stimulation with AngII. At ~6 h after H_2O_2 treatment, cellular distribution of cytochrome *c* was visualized by immunostaining. Images shown represent similar results obtained from three independent experiments. *F* and *G*, the amounts of H_2O_2- (*F*) or etoposide- (*G*) induced DNA fragmentation in the absence or presence of stimulation with AngII were measured as described under "Experimental Procedures." Values were expressed as folds over basal in non-stimulated, non-treated (*NT*), CTL-siRNA-transfected cells and represent the mean ± S.E. from at least six independent experiments. *H–J*, VSMCs were stimulated with SII prior to treatment with either H_2O_2 or etoposide as indicated. The amounts of cleaved caspase-3 (*H* and *I*) and fragmented DNA (*J*) were determined and expressed as described above. Data represent the mean ± S.E. from at least 5 (*I*) or 6 (*J*) independent experiments. All statistical analyses were performed as described under "Experimental Procedures."

that RSK- and AKT-mediated phosphorylation of BAD are required for AngII-stimulated, β-arrestin-2-mediated cytoprotective processes. Furthermore, the results are consistent with the findings shown above (Fig. 3, *A–D*) that both activities of RSK and AKT are essential for AngII-stimulated protection from apoptotic stimuli.

The AT_{1A}R-stimulated ERK-RSK-BAD Phosphorylation Cascade in HEK-293 Cells Is Also Mediated by β-Arrestin-2—Phosphorylation of BAD is thought to control its apoptotic activity by regulating its functionally antagonistic binding to anti-apoptotic proteins such as Bcl-xL (dephosphorylated form) (11, 20) or the scaffold protein 14-3-3 (phosphorylated form) (19). Accordingly, we wished to determine the effects of β-arrestin-2-mediated phosphorylation of BAD on its binding to Bcl-xL and 14-3-3. However, we were unable to detect the interaction of these proteins expressed at physiological levels in VSMCs with our co-immunoprecipitation assay. Alternatively, we found that we were able to perform such experiments with these proteins endogenously expressed in HEK-293 cells expressing the AT_{1A} receptor. However, such experiments are only relevant to the situation in VSMCs if the signaling pathway we have identified in the VSMCs also operates in the HEK-293 cells. As shown in Fig. 4, *A–C*, in HEK-293 cells stably transfected with a plasmid expressing the AT_{1A} receptor, AngII provokes a protracted activation (assessed by phosphorylation of Thr^{359}/Ser^{363}) of p90RSK. Two different β-arrestin-2 siRNAs (Fig. 4*A*) inhibit this response (Fig. 4*B*), but only at times after 5 min of stimulation (Fig. 4*C*). In contrast, the protein kinase C (PKC) inhibitor Ro31-8425 or GF109203X, which has been shown in HEK-293 cells to block G protein-dependent ERK activation by AngII (21, 22), inhibits the early component of p90RSK activation (Fig. 4*C*). Confirming that virtually all of the AngII-induced phosphorylation of p90RSK at Thr^{359} and Ser^{363} is mediated by ERK, the MEK inhibitor U0126 completely abolishes the p90RSK phosphorylation response (Fig. 4*C*). These patterns of sensitivities to PKC blockade and β-arrestin-2 siRNA directly parallel our previous find-

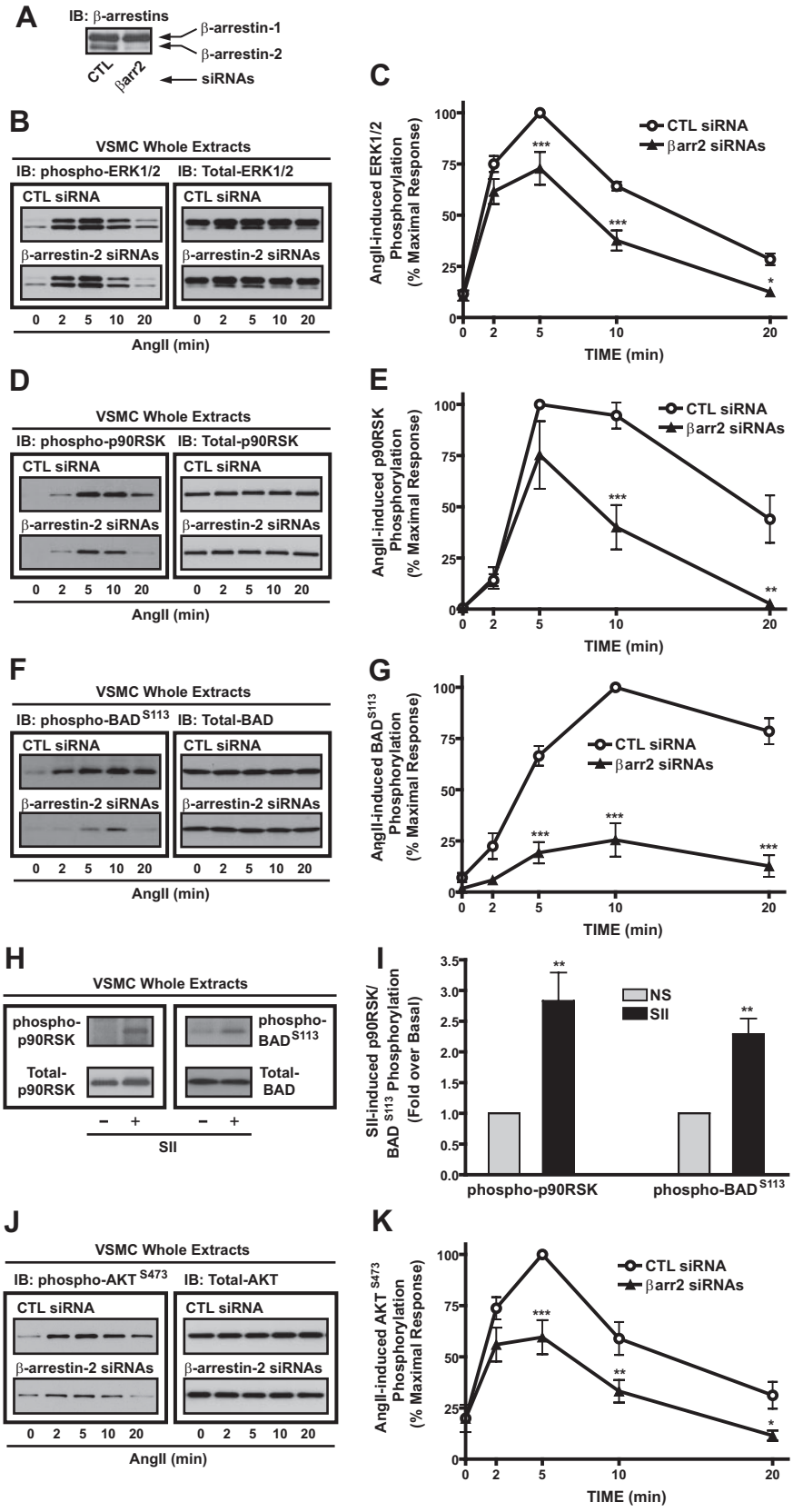

ings for AngII-stimulated phosphorylation of ERK in these cells (22).

Despite this evidence that β-arrestin-2-mediated ERK activation accounts for only the later (>5 min) occurring phosphorylation of p90RSK, the data in Fig. 4, *D* and *E*, suggest that, as in the VSMCs, almost all of the downstream phosphorylation of BAD by RSK is mediated by the pool of p90RSK, which is activated through β-arrestin-dependent ERK. After β-arrestin-2 siRNA transfection, there is almost complete loss of the AngII-stimulated BAD phosphorylation at Ser^{75}, the homologous site of Ser^{113} in human BAD (Fig. 4, *D* and *E*). As expected, virtually all the BAD phosphorylation at this site is also blocked by the selective RSK inhibitor SL0101 and MEK inhibitor U0126 (Fig. 4*E*). Because PKC inhibitors have been shown to efficiently block RSK, which belongs to the same AGC kinase family as PKC (42), their effects on BAD phosphorylation could not be reliably studied.

To further validate the G protein-independent nature of the phosphorylation of p90RSK and BAD, we stimulated HEK-293 cells expressing the AT_{1A} receptor with SII. As shown in Fig. 4, *F* and *G*, this stimulation leads to prolonged increases in both p90RSK and BAD phosphorylation. Taken together, results in Fig. 4 confirm that the AT_1R-β-arrestin-2-ERK-p90RSK-BAD pathway delineated in rat VSMCs (Fig. 2) is also operative in HEK-293 cells.

β-Arrestin-2 Regulates Interactions of BAD with Its Partners upon AngII Stimulation—As noted above, the dynamic interactions of BAD with its partners regulate the pro-apoptotic function of BAD (11, 19, 20). Our results demonstrate that BAD phosphorylation by RSK is mediated predominantly by β-arrestin-2-dependent signaling (Figs. 2*G* and 4*E*) and also suggest that its phosphorylation by AKT is partially dependent on β-arrestin-2 (Fig. 2*K*). Accordingly, we examined BAD interactions with its partners at their endogenous levels upon AngII stimulation in control or β-arrestin-2 siRNA-transfected HEK-293 cells stably expressing AT_{1A} receptors. Stimulation with AngII leads to a significant increase in the amount of BAD present in 14-3-3 protein immunoprecipitates in control cells (Fig. 5, *A* and *B*). In parallel, the quantity of the 14-3-3 protein co-immunoprecipitated with BAD is augmented by AT_{1A} receptor activation (Fig. 5, *C* and *D*). AT_{1A}R-mediated increases in the interaction of BAD with 14-3-3 shown by both BAD and 14-3-3 immunoprecipitation are eliminated in β-arrestin-2 siRNA-transfected cells (Fig. 5, *A–D*). Conversely, we found that AngII stimulation decreases the interaction of BAD with Bcl-xL. Fig. 5, *E* and *F*, show the reduced amount of Bcl-xL in BAD immunoprecipitates upon AngII stimulation in control cells. This reduction is not observed in β-arrestin-2 siRNA-transfected cells. Fig. 5, *G* and *H*, show that in the HEK-293 cell lysates used in these experiments, AngII-stimulated BAD phosphorylation at the RSK site (Ser^{75}) is completely abolished by β-arrestin-2 siRNA, as shown in Fig. 4*E*. Taken together, these results demonstrate that activation of AT_1 receptors leads to a β-arrestin-2-dependent increase in BAD interaction with 14-3-3 and a decrease in its association with Bcl-xL, resulting in an anti-apoptotic signal. Moreover, the results strongly suggest that AngII-stimulated changes in BAD complex formation are mediated by p90RSK and AKT phosphorylation of BAD in a β-arrestin-2-dependent manner.

DISCUSSION

The present study shows that β-arrestin-2 plays a crucial role in AngII-stimulated anti-apoptotic responses and delineates the downstream biochemical pathways responsible for this AngII-stimulated, β-arrestin-2-mediated cytoprotection from apoptotic challenge. Upon stimulation with AngII, the pro-apoptotic protein BAD is phosphorylated through two signaling pathways, ERK-p90RSK and PI3K-AKT. Activation of both pathways appears to be β-arrestin-2-dependent. This β-arrestin-2-dependent BAD phosphorylation leads to increases in BAD-14-3-3 association and decreases in the interaction of BAD with Bcl-xL. Such changes in the association of BAD with its partners lead to attenuation of its pro-apoptotic function, resulting in AngII-stimulated protection from apoptotic challenges. There have been reports implicating β-arrestins in both pro- and anti-apoptotic responses as well as in non-apoptotic cell death (3–10). However, the biochemical pathways through which β-arrestins mediate these responses upon 7TMR activation have not been delineated. The results reported here establish a downstream molecular mechanism by which β-arrestin-2 mediates anti-apoptosis in response to activation of the physiologically important AT_1 receptor in a non-transfected natural cell, VSMC.

β-Arrestin-mediated, but G protein-independent, activation of ERK1/2 has been a focus of study for the functions of β-arrestins as signal transducers for 7TMR activation (2, 21–25). In the case of AT_{1A}R-mediated ERK activation, it has been demonstrated that upon activation of the receptor, β-arrestin-2 scaffolds the components of the ERK cascade, Raf-1, MEK1, and ERK1/2, into the receptor complex, leading to activation of ERK1/2 (2, 43). In addition, we have previously shown that β-arrestin-2-dependent activation displays distinct temporal and spatial patterns from those due to G protein-dependent activation (22). In particular, ERK activated via the β-arrestin-2-dependent pathway is confined to the cytoplasm, whereas ERK activated via G proteins translocates into the nucleus (22,

FIGURE 2. **Effects of silencing β-arrestin-2 expression on ERK-RSK-BAD phosphorylation as well as AKT activation in response to AngII in rat VSMCs.** *A–G*, indicated siRNA-transfected VSMCs were serum-starved for ~24 h and then stimulated with 100 nM AngII at 37 °C for the indicated periods. After stimulation, expression of β-arrestins (*A*) and phosphorylation of ERK1/2 (*B*), p90RSK at Thr^{359}/Ser^{363} (*D*), and BAD at Ser^{113} (*F*) were visualized by immunoblotting (*IB*). *C*, contents of ERK1/2 phosphorylation in the immunoblots (*left panels*) were quantified and normalized by the amount of total ERK1/2 (*right panels*). Values were expressed as percent of the maximal phosphorylation of ERK1/2 obtained in control (*CTL*) siRNA-transfected cells. Data were obtained from five independent experiments. *E* and *G*, the amounts of p90RSK (*E*) and BAD (*G*) phosphorylation shown in the immunoblots were measured and determined as described for *C*. Data were obtained from six independent experiments. *H* and *I*, serum-starved VSMCs were stimulated with 10 μM SII for 5 min. The level of SII-induced p90RSK and BAD phosphorylation were determined as described above and expressed folds over basal phosphorylation in non-stimulated (*NS*) cells. Values were obtained from seven independent experiments (*I*). *J* and *K*, siRNA-transfected VSMCs were serum-starved and then stimulated with 100 nM AngII for the indicated periods. AKT phosphorylation at Ser^{473} was visualized (*J*) and determined (*K*) as described for *C* from six independent experiments. In all graphs, each data point represents the mean ± S.E., and statistical analyses were carried out as described under "Experimental Procedures."

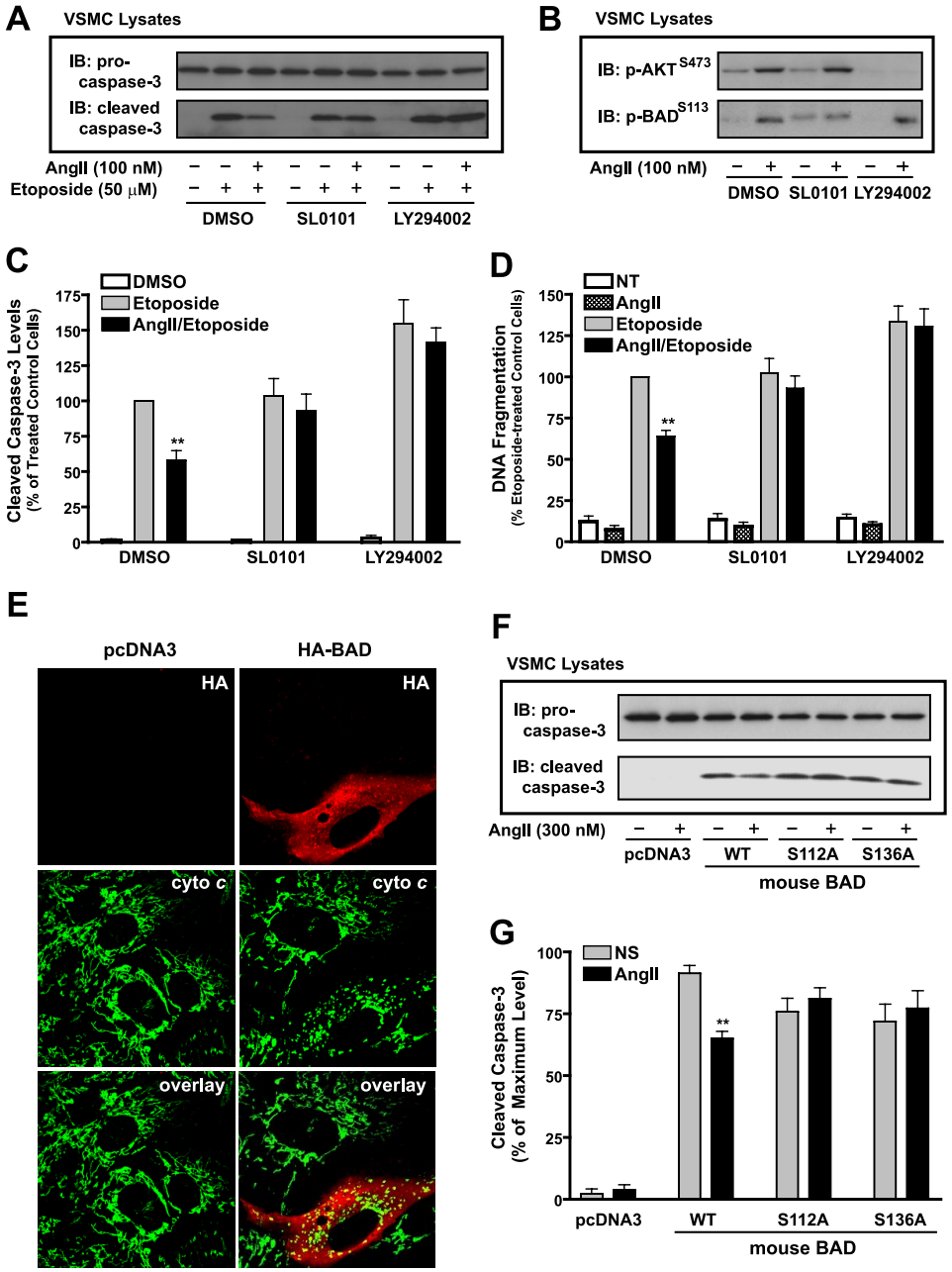

FIGURE 3. **Kinase activities of both RSK and AKT as well as BAD phosphorylation are required for AngII-promoted cellular protection in rat VSMCs.** *A–D*, serum-starved VSMCs were incubated with either 100 μM SL0101 for 2 h or 1 μM LY294004 for 1 h at 37 °C before stimulation with AngII and following etoposide treatment. *A* and *C*, contents of pro- and cleaved caspase-3 were visualized (*A*), and the amounts of cleaved caspase-3 were determined (*C*) as described in the legend to Fig. 1. Values were expressed as percent of the level obtained in vehicle alone (dimethyl sulfoxide, *DMSO*) and then etoposide-treated cells in the absence of stimulation with AngII and represent the mean ± S.E. from seven independent experiments (*C*). *B*, after stimulation with AngII for 5 min, phosphorylation of AKT at Ser^{473} and BAD at Ser^{113} were visualized by immunoblotting (*IB*). *D*, levels of fragmented DNA were measured and expressed as described for *C*. Data represent the mean ± S.E. from seven independent experiments. *E–G*, VSMCs were transfected with each plasmid expressing the indicated BAD. Empty pcDNA3 was used as a transfection control. *E*, cells were treated with 50 μM Z-VAD-fmk during transfection. Within 24 h after transfection, cellular distribution of cytochrome *c* (*green*) and expression of hemagglutinin-tagged BAD (*red*) were visualized by immunostaining. Images shown represent similar results obtained from four independent experiments. *F*, approximately 6 h after transfection, cells were stimulated with 300 nM AngII and incubated overnight. Contents of pro- and cleaved caspase-3 were visualized by immunoblotting. *G*, the amounts of cleaved caspase-3 were measured and expressed as percent of the maximum level obtained from each 10 independent experiment. Values represent the mean ± S.E. All statistical analyses were carried out as described under "Experimental Procedures."

26). These distinct patterns strongly suggest that the substrates of ERK activated via β-arrestin-2-mediated signaling may be largely cytoplasmic. Cytoplasmic ERK activity appears to be important in the regulation of cell morphology, migration, and viability (2, 22). However, very little is known about how phosphorylation of cytoplasmic ERK substrates, downstream of β-arrestin signaling, regulates cellular responses. The only known example is the very recent finding that β-arrestin-2-mediated ERK activation by the AT_1 receptor leads to an increase in protein synthesis via activation of a downstream kinase, Mnk1 (32). The present study reveals anti-apoptosis mediated by BAD phosphorylation as another downstream response of β-arrestin-mediated ERK signaling stimulated by a 7TMR. These results thus expand our understanding of the roles of β-arrestin in determining the physiological outcomes of signaling initiated from 7TMRs.

Besides ERK1/2, β-arrestins have been implicated in the regulation of various other signaling molecules. These include other MAPKs, JNK3, and p38 as well as c-Src, PI3K, AKT, and RhoA (2). Most of these molecules have been shown to be involved in regulation of apoptosis. In the case of AKT for example, it has been reported that deficiency of β-arrestins 1 and 2 leads to loss of AKT activation and anti-apoptotic effects following insulin-like growth factor 1 stimulation in mouse embryonic fibroblasts (6). Although there has been a report showing β-arrestin-1-dependent AKT activation in response to thrombin mediated through 7TM protease-activated receptors (27), its function in apoptosis was not studied. Our present data show that stimulation of the AT_1 receptor leads to AKT activation in a β-arrestin-2-dependent manner (Fig. 2, *J* and *K*). Our results also demonstrate that the activity of PI3K, the upstream kinase of AKT, is required for AngII-stimulated protection from apoptotic challenges in VSMCs (Fig.

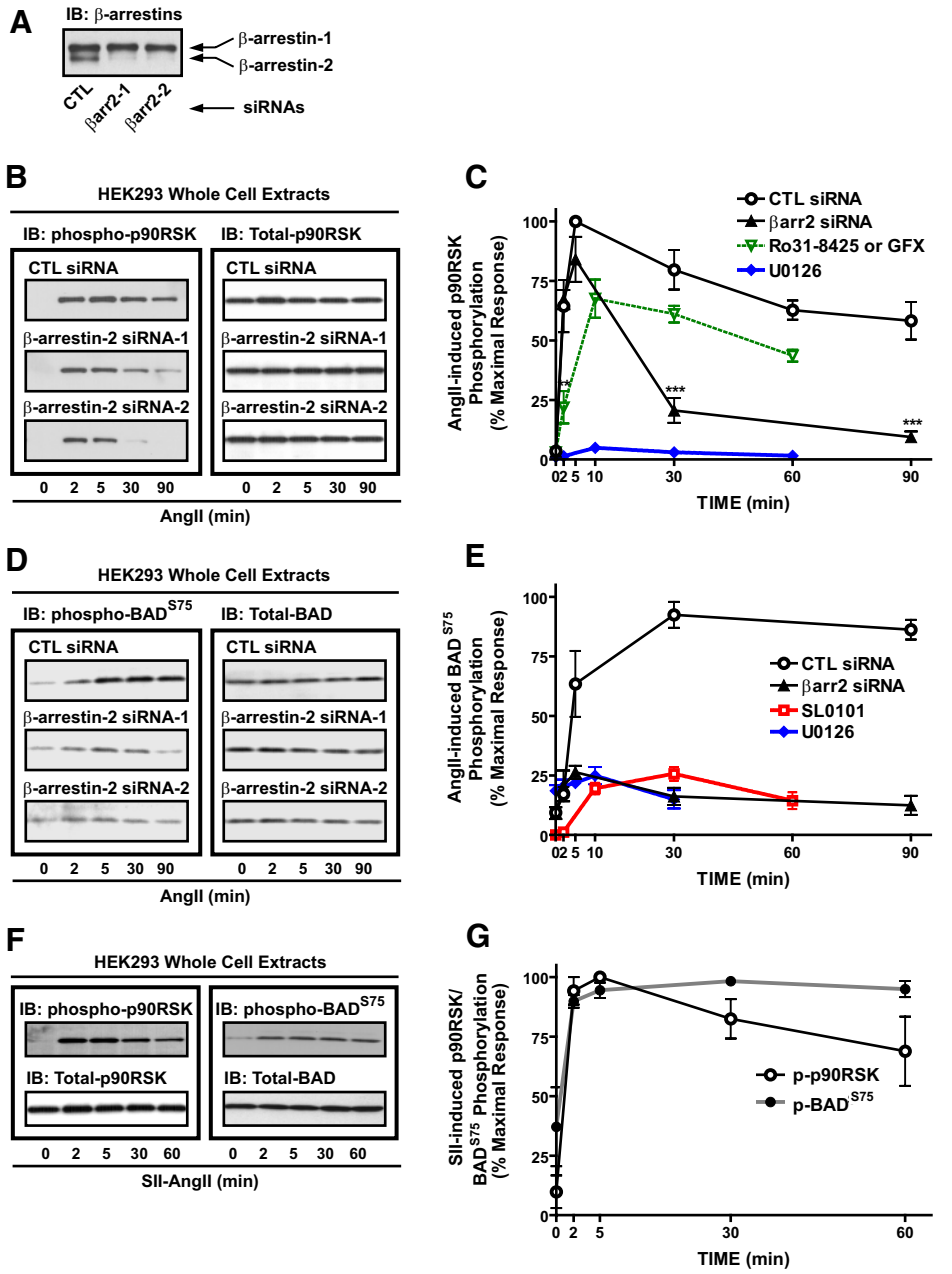

FIGURE 4. **β-Arrestin-2 also mediates the ERK-RSK-BAD phosphorylation cascade upon stimulation of the AT_{1A} receptor stably expressed in HEK-293 cells.** *A–E*, cells were transfected with the indicated siRNAs and serum starved for ~6 h. During starvation, inhibitors were pre-treated before stimulation: 1 μM Ro31-8425, 2.5 μM GF109203X (*GFX*), and 5 μM U0126 for 30 min; 100 μM SL0101 for 2 h. After stimulation with 100 nM AngII at 37 °C for the indicated periods, whole cell extracts were prepared to visualize expression β-arrestins (*A*) and phosphorylation of p90RSK at Thr^{359}/Ser^{363} (*B*) and BAD at Ser^{75} (*D*) by immunoblotting (*IB*). Levels of p90RSK (*C*) and BAD (*D*) phosphorylation in each sample were determined as described for Fig. 2 and expressed as percent of the maximal phosphorylation in control (*CTL*) siRNA-transfected cells. Data were obtained from at least three independent experiments. *F* and *G*, serum-starved $AT_{1A}R$-expressing HEK-293 cells were stimulated with 10 μM SII for the indicated periods. Contents of p90RSK (*left panel*) and BAD (*right panel*) phosphorylation were visualized (*F*) and determined (*G*). Levels of phosphorylation in each time point were expressed as percent of the maximal phosphorylation obtained in three independent experiments (*G*). In all graphs, each data point represents the mean ± S.E. and statistical analyses were carried out as described under "Experimental Procedures."

We show that p90RSK is a kinase that transfers the β-arrestin-mediated ERK activation signal to anti-apoptotic effects in response to AT_1 receptor activation. RSK is a well known ERK substrate and mediates signals to many cellular responses, including cell survival, through phosphorylation of its downstream targets (40, 41). One such target is BAD, which RSK phosphorylates at serine 113 (in the case of rat BAD) (14–16). In addition to RSK, PKA and AKT have been considered as putative upstream kinases for BAD phosphorylation (16, 17, 44). Nonetheless, our data show that inhibition of either ERK or RSK, but not PI3K activities completely abolishes phosphorylation of BAD at this site following activation of the AT_1 receptor (Figs. 3*B* and 4*E*). Such data clearly demonstrate that BAD phosphorylation at Ser^{113} in response to AT_1 receptor activation is mediated through the ERK-RSK pathway. In addition to the ERK-RSK-BAD pathway, our data show that blockade of the PI3K-AKT pathway also eliminates AngII-stimulated anti-apoptosis (Fig. 3, *C* and *D*). However, this PI3K/AKT-dependent anti-apoptotic effect must be mediated through phosphorylation of BAD at a different site, *e.g.* Ser^{136} (17, 18) or possibly phosphorylation of other targets (45).

Our data show that knocking-down β-arrestin-2 expression leads to almost complete inhibition in RSK-mediated phosphorylation of BAD following AT_1 receptor activation (Figs. 2, *F* and *G*, and 4, *D* and *E*), suggesting that this process may be entirely β-arrestin-2-mediated. These results are quite interesting in view of the previous and present findings that ERK activation in response to stimulation of the AT_1 receptor is mediated both by independent β-arrestin-2- and G protein-mediated signaling pathways (21, 22). The data presented here also show that activation of p90RSK, the kinase that transfers signals from activated ERK to BAD phosphorylation, is mediated through these two pathways (Fig. 2, *D* and *E*, and 4, *B* and *C*). Furthermore, we have previously demonstrated that PKC activity is essential for G protein-

3, *C* and *D*). As described above, β-arrestin might regulate apoptotic processes through multiple mechanisms. In fact, the present study indicates that β-arrestin-2 mediates the anti-apoptotic response to AngII through two different pathways, ERK-RSK and PI3K-AKT.

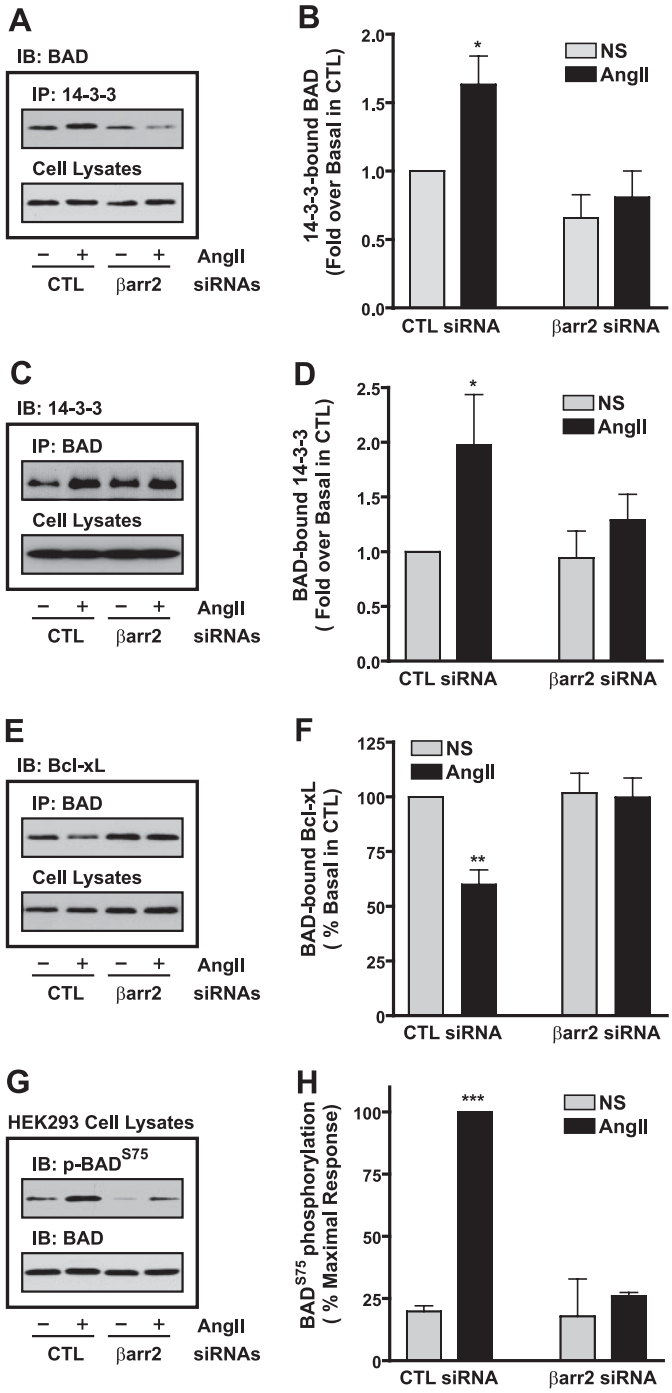

FIGURE 5. **Effects of β-arrestin-2 knocking down on AngII-induced interaction of BAD with its partners in AT_{1A}R-stably expressing HEK-293 cells.** Cells were transfected with either control (*CTL*) or β-arrestin-2 (*βarr2*) siRNA. After transfection, cells were serum-starved for ~6 h and then stimulated with 100 nM AngII for 30 min. *A*, cell lysates were prepared and used for immunoprecipitation (*IP*) with a 14-3-3 antibody. The BAD protein co-immunoprecipitated with 14-3-3 was visualized by immunoblotting (*IB*) (*upper blot*), and its amount in each sample was quantified and normalized by the amounts of BAD in input lysates (*lower blot*). *B*, values were expressed as folds over the basal level obtained in non-stimulated (*NS*), CTL siRNA-transfected cells. Data were obtained from four independent experiments. *C–F*, after immunoprecipitation with a BAD antibody, co-immunoprecipitated 14-3-3 (*C*) and Bcl-xL (*E*) proteins with BAD were visualized, and their amounts were determined as described for *A*. *D*, data were expressed as folds over the basal level and obtained from three independent experiments. *F*, values were expressed as percent of the basal level and obtained from four independent experiments. *G* and *H*, phosphorylation of BAD at Ser^{75} in each lysate used for immunoprecipitation experiments were visualized (*G*) and measured (*H*). Data were expressed as percent of the response to AngII in CTL siRNA-transfected cells and obtained from four independent experiments (*H*). In all graphs, values represent the mean ± S.E., and statistical analyses were carried out as described under "Experimental Procedures."

dependent, but not β-arrestin-mediated signaling to ERK activation following stimulation of the AT_{1A} receptor (21, 22). There have been reports that PKC is involved in RSK-mediated BAD phosphorylation (46, 47), implying that G protein-dependent signaling might be involved. However, we found that SII, a mutant ligand that fails to activate G proteins, induces BAD phosphorylation by RSK (Figs. 2, *H* and *I*, and 4, *F* and *G*) as well as promotes anti-apoptotic effects (Fig. 1, *H–J*). This strongly supports the contention that AT_1R-mediated BAD phosphorylation via the ERK-RSK pathway in VSMCs as well as HEK-293 cells is G protein-independent. Furthermore, we have previously shown that restriction of activated ERK to the cytoplasm, where BAD resides (13), is one of the striking characteristics of β-arrestin-, but not G protein-dependent ERK activation (22, 26). Consequently, AT_1R-induced phosphorylation of BAD by RSK provides an example of how an appreciation of the distinct characteristics of β-arrestin *versus* G protein signaling can illuminate issues of apparent "compartmentalization" of cellular signaling events.

Apoptosis of VSMCs plays a significant role in vascular remodeling as well as in vascular diseases, including atherosclerosis and neointima formation after injury, which are also associated with cell proliferation (34, 48, 49). AngII is a well known cell survival factor for VSMCs (28, 29, 34). Our data establish a mechanism by which AngII leads to cellular protection as well as demonstrate that β-arrestin-2 is a key mediator of this mechanism. Our results thus suggest that β-arrestin-2 may play an important role in vascular diseases and remodeling, and raise the possibility that β-arrestins may represent a therapeutic target in such diseases. Several previous findings support this idea. Atherosclerotic human coronary arteries show up-regulated (~2-fold higher) β-arrestin-2 mRNA levels compared with normal human coronary arteries (50). β-Arrestin-2 appears to be the predominant β-arrestin isoform in the atherosclerotic lesion (48). Moreover, deficiency of β-arrestin-2 leads to reduced aortic atherosclerosis and a decrease in the prevalence of atheroma SMCs in low density lipoprotein receptor-deficient mice (48). In agreement with our results, it also has been reported that β-arrestin-2 knock-out mice show augmented medial SMC apoptosis in carotid arteries after endothelial denudation to induce neointimal hyperplasia (48). Furthermore, ERK and AKT activation in SMCs of injured arteries is reduced in β-arrestin-2 knock-out mice compared with wild-type animals (48).

In summary, the present study reveals anti-apoptosis as a physiological consequence of β-arrestin-mediated signaling upon activation of the 7TM AT_1 receptor, and delineates the β-arrestin-2-mediated anti-apoptotic pathways. These results also provide better understanding of the role of β-arrestin-2 in apoptosis-related vascular diseases at the molecular level and may allow the development of therapeutic agents that target the β-arrestins for such diseases.

Acknowledgments—We thank Dr. Jeffrey J. Kovacs for critical reading of the manuscript and helpful comments. We also thank Donna Addison and Elizabeth Hall for excellent secretarial assistance.

REFERENCES

1. Hall, R. A., Premont, R. T., and Lefkowitz, R. J. (1999) *J. Cell Biol.* **145,** 927–932
2. DeWire, S. M., Ahn, S., Lefkowitz, R. J., and Shenoy, S. K. (2007) *Annu. Rev. Physiol.* **69,** 483–510
3. Shi, Y., Feng, Y., Kang, J., Liu, C., Li, Z., Li, D., Cao, W., Qiu, J., Guo, Z., Bi, E., Zang, L., Lu, C., Zhang, J. Z., and Pei, G. (2007) *Nat. Immunol.* **8,** 817–824
4. Zhao, M., Wimmer, A., Trieu, K., Discipio, R. G., and Schraufstatter, I. U. (2004) *J. Biol. Chem.* **279,** 49259–49267
5. Revankar, C. M., Vines, C. M., Cimino, D. F., and Prossnitz, E. R. (2004) *J. Biol. Chem.* **279,** 24578–24584
6. Povsic, T. J., Kohout, T. A., and Lefkowitz, R. J. (2003) *J. Biol. Chem.* **278,** 51334–51339
7. DeFea, K. A., Vaughn, Z. D., O'Bryan, E. M., Nishijima, D., Dery, O., and Bunnett, N. W. (2000) *Proc. Natl. Acad. Sci. U. S. A.* **97,** 11086–11091
8. Luan, B., Zhang, Z., Wu, Y., Kang, J., and Pei, G. (2005) *EMBO J.* **24,** 4237–4246
9. Wang, P., Gao, H., Ni, Y., Wang, B., Wu, Y., Ji, L., Qin, L., Ma, L., and Pei, G. (2003) *J. Biol. Chem.* **278,** 6363–6370
10. Castro-Obregon, S., Rao, R. V., del Rio, G., Chen, S. F., Poksay, K. S., Rabizadeh, S., Vesce, S., Zhang, X. K., Swanson, R. A., and Bredesen, D. E. (2004) *J. Biol. Chem.* **279,** 17543–17553
11. Adams, J. M., and Cory, S. (2007) *Oncogene* **26,** 1324–1337
12. Datta, S. R., Ranger, A. M., Lin, M. Z., Sturgill, J. F., Ma, Y. C., Cowan, C. W., Dikkes, P., Korsmeyer, S. J., and Greenberg, M. E. (2002) *Dev. Cell* **3,** 631–643
13. Bergmann, A. (2002) *Dev. Cell* **3,** 607–608
14. Bonni, A., Brunet, A., West, A. E., Datta, S. R., Takasu, M. A., and Greenberg, M. E. (1999) *Science* **286,** 1358–1362
15. Shimamura, A., Ballif, B. A., Richards, S. A., and Blenis, J. (2000) *Curr. Biol.* **10,** 127–135
16. Yang, X., Liu, L., Sternberg, D., Tang, L., Galinsky, I., DeAngelo, D., and Stone, R. (2005) *Cancer Res.* **65,** 7338–7347
17. del Peso, L., Gonzalez-Garcia, M., Page, C., Herrera, R., and Nunez, G. (1997) *Science* **278,** 687–689
18. Datta, S. R., Dudek, H., Tao, X., Masters, S., Fu, H., Gotoh, Y., and Greenberg, M. E. (1997) *Cell* **91,** 231–241
19. Datta, S. R., Katsov, A., Hu, L., Petros, A., Fesik, S. W., Yaffe, M. B., and Greenberg, M. E. (2000) *Mol. Cell* **6,** 41–51
20. Yang, E., Zha, J., Jockel, J., Boise, L. H., Thompson, C. B., and Korsmeyer, S. J. (1995) *Cell* **80,** 285–291
21. Wei, H., Ahn, S., Shenoy, S. K., Karnik, S. S., Hunyady, L., Luttrell, L. M., and Lefkowitz, R. J. (2003) *Proc. Natl. Acad. Sci. U. S. A.* **100,** 10782–10787
22. Ahn, S., Shenoy, S. K., Wei, H., and Lefkowitz, R. J. (2004) *J. Biol. Chem.* **279,** 35518–35525
23. Ren, X. R., Reiter, E., Ahn, S., Kim, J., Chen, W., and Lefkowitz, R. J. (2005) *Proc. Natl. Acad. Sci. U. S. A.* **102,** 1448–1453
24. Gesty-Palmer, D., Chen, M., Reiter, E., Ahn, S., Nelson, C. D., Wang, S., Eckhardt, A. E., Cowan, C. L., Spurney, R. F., Luttrell, L. M., and Lefkowitz, R. J. (2006) *J. Biol. Chem.* **281,** 10856–10864
25. Shenoy, S. K., Drake, M. T., Nelson, C. D., Houtz, D. A., Xiao, K., Madabushi, S., Reiter, E., Premont, R. T., Lichtarge, O., and Lefkowitz, R. J. (2006) *J. Biol. Chem.* **281,** 1261–1273
26. Tohgo, A., Pierce, K. L., Choy, E. W., Lefkowitz, R. J., and Luttrell, L. M. (2002) *J. Biol. Chem.* **277,** 9429–9436
27. Goel, R., Phillips-Mason, P. J., Raben, D. M., and Baldassare, J. J. (2002) *J. Biol. Chem.* **277,** 18640–18648
28. Mehta, P. K., and Griendling, K. K. (2007) *Am. J. Physiol.* **292,** C82–C97
29. Nakashima, H., Suzuki, H., Ohtsu, H., Chao, J. Y., Utsunomiya, H., Frank, G. D., and Eguchi, S. (2006) *Curr. Vasc. Pharmacol.* **4,** 67–78
30. Holloway, A. C., Qian, H., Pipolo, L., Ziogas, J., Miura, S., Karnik, S., Southwell, B. R., Lew, M. J., and Thomas, W. G. (2002) *Mol. Pharmacol.* **61,** 768–777
31. Attramadal, H., Arriza, J. L., Aoki, C., Dawson, T. M., Codina, J., Kwatra, M. M., Snyder, S. H., Caron, M. G., and Lefkowitz, R. J. (1992) *J. Biol. Chem.* **267,** 17882–17890
32. DeWire, S. M., Kim, J., Whalen, E. J., Ahn, S., Chen, M., and Lefkowitz, R. J. (2008) *J. Biol. Chem.* **283,** 10611–10620
33. Ahn, S., Wei, H., Garrison, T. R., and Lefkowitz, R. J. (2004) *J. Biol. Chem.* **279,** 7807–7811
34. Mallat, Z., and Tedgui, A. (2000) *Br. J. Pharmacol.* **130,** 947–962
35. Pollman, M. J., Yamada, T., Horiuchi, M., and Gibbons, G. H. (1996) *Circ. Res.* **79,** 748–756
36. Lee, M. H., El-Shewy, H. M., Luttrell, D. K., and Luttrell, L. M. (2008) *J. Biol. Chem.* **283,** 2088–2097
37. Fabregat, I., Roncero, C., and Fernandez, M. (2007) *Liver Int.* **27,** 155–162
38. Desagher, S., and Martinou, J. C. (2000) *Trends Cell Biol.* **10,** 369–377
39. Sun, M. G., Williams, J., Munoz-Pinedo, C., Perkins, G. A., Brown, J. M., Ellisman, M. H., Green, D. R., and Frey, T. G. (2007) *Nat. Cell Biol.* **9,** 1057–1065
40. Frodin, M., and Gammeltoft, S. (1999) *Mol. Cell. Endocrinol.* **151,** 65–77
41. Hauge, C., and Frodin, M. (2006) *J. Cell Sci.* **119,** 3021–3023
42. Davies, S. P., Reddy, H., Caivano, M., and Cohen, P. (2000) *Biochem. J.* **351,** 95–105
43. Luttrell, L. M., Roudabush, F. L., Choy, E. W., Miller, W. E., Field, M. E., Pierce, K. L., and Lefkowitz, R. J. (2001) *Proc. Natl. Acad. Sci. U. S. A.* **98,** 2449–2454
44. Harada, H., Becknell, B., Wilm, M., Mann, M., Huang, L. J., Taylor, S. S., Scott, J. D., and Korsmeyer, S. J. (1999) *Mol. Cell* **3,** 413–422
45. Parcellier, A., Tintignac, L. A., Zhuravleva, E., and Hemmings, B. A. (2008) *Cell. Signal.* **20,** 21–30
46. Lee, K. W., Kim, S. G., Kim, H. P., Kwon, E., You, J., Choi, H. J., Park, J. H., Kang, B. C., Im, S. A., Kim, T. Y., Kim, W. H., and Bang, Y. J. (2008) *Cancer Res.* **68,** 1916–1926
47. Tan, Y., Ruan, H., Demeter, M. R., and Comb, M. J. (1999) *J. Biol. Chem.* **274,** 34859–34867
48. Kim, J., Zhang, L., Peppel, K., Wu, J. H., Zidar, D. A., Brian, L., DeWire, S. M., Exum, S. T., Lefkowitz, R. J., and Freedman, N. J. (2008) *Circ. Res.* **103,** 70–79
49. Korshunov, V. A., and Berk, B. C. (2008) *Curr. Opin. Hematol.* **15,** 250–254
50. Archacki, S. R., Angheloiu, G., Tian, X. L., Tan, F. L., DiPaola, N., Shen, G. Q., Moravec, C., Ellis, S., Topol, E. J., and Wang, Q. (2003) *Physiol. Genomics* **15,** 65–74